INTERNATIONAL JOURNAL FOR NUMERICAL METHODS IN FLUIDS
Int. J. Numer. Meth. Fluids **28**: 1303–1324 (1998)

AUTOMATIC GRID GENERATION OF COMPLEX GEOMETRIES IN CARTESIAN CO-ORDINATES

WANLAI LIN AND CHING JEN CHEN*

Department of Mechanical Engineering, FAMU-FSU College of Engineering, Florida A&M University and Florida State University, 2525 Pottsdamer St., Tallahassee, FL 32310-6046, USA

SUMMARY

A method of automatic grid generation for complex boundaries in Cartesian co-ordinates is proposed in this paper. In addition to the Cartesian grid lines the diagonal segments are used for the approximations of complex geometries in Cartesian co-ordinates. A structured Cartesian grid is employed for the sake of the numerical simplicity and the potential of automatic grid generation. The automatic grid generation is achieved by this diagonal Cartesian method and the accuracy estimations of geometry approximations are given. The approximations of a few complex geometries, such as the multibody system in porous media, lake banks, grooved channels and spheres are shown and analyzed. The proposed method is verified by the numerical solutions of a rotated cavity flow. It is shown that the diagonal Cartesian method improves both the accuracy of geometry approximations and the numerical solution of a rotated cavity flow, comparing with the traditional saw-tooth method in which only Cartesian grid lines are utilized for geometry approximations. The stability and convergence of the proposed method is demonstrated. Finally, the application of the diagonal Cartesian method for the prediction of a grooved channel flow is presented. © 1998 John Wiley & Sons, Ltd.

KEY WORDS: grid generation; automation; Cartesian; diagonal; saw-tooth

1. INTRODUCTION

Due to recent advances in high performance computers, the numerical simulation of fluid flows and heat transfer problems has become common and is possible in practical applications. In the computational simulation, it is important to accurately approximate the boundary contour because the boundary conditions on the body shapes play an important role in the accurate simulation of fluid flows and heat transfer. For regular geometries, good results can be obtained with current numerical techniques. However, the simulation of flows and heat transfer around complex geometries remains a challenging task, as it is still difficult to generate a grid system in which the complex boundary conditions can be satisfied and the numerical solution is simple, accurate and stable. This is particularly so when the solid object is three-dimensional. The difficulty in generating a computational grid for a problem with complex geometry lies in making the grid understand where the boundary surfaces are. The first step in the numerical computation is to obtain a geometric description of the various surfaces, e.g. by converting CAD files into the numerical grid representation. This process

* Correspondence to: Department of Mechanical Engineering, FAMU-FSU College of Engineering, Florida A&M University and Florida State University, 2525 Pottsdamer Street, Tallahassee, FL 32310-6046, USA. Tel: +1 850 4876439; Fax: +1 850 4876486; E-mail: wlin@scri.fsu.edu or cjchen@eng.fsu.edu

CCC 0271–2091/98/191303–22$17.50

Received February 1997
Revised January 1998

itself can be very time-consuming. The second step invokes the creation of the actual computational grid around the body. This can be very tricky, even for an inviscid flow, because it not only involves accuracy of the solutions, but also the stability. The boundary-fitted co-ordinate system proposed by Thompson [1] is a popular choice because the boundary surface is fitted with a new co-ordinate line based on the body contour. This approach clearly requires additional effort in generating the new co-ordinate for every object and solving, in general, more complex governing equations on the boundary-fitted co-ordinate. If the problem has sharp boundaries or complex multibody systems, it is difficult to achieve automatic grid generation with the boundary-fitted co-ordinates. In fact, automation of the generation of boundary-fitted grids for problems with complex geometries is not currently possible. Current algorithms for boundary-fitted co-ordinates are still problem-dependent and require much human–machine interaction for such problems. It has been estimated that up to 80% of the total simulation efforts is needed on the grid generation for problems involving complex boundaries [2].

The unstructured mesh system, which is traditionally developed for the FE (finite element) method [3], offers another alternative in numerical grid systems. It uses both triangular and quadrilateral elements, so that complex geometries can be approximated by a series of linear or splined segments. Additional efforts are required to solve the system of discretized equations generated by these methods because the grids are unstructured. The computation, in general, consumes more CPU time as it requires additional computer memory in order to identify the nodal locations. It also requires the proper sequencing of the nodes in the numerical solution. Overset grids, such as Chimera, have great versatility and are especially attractive for multibody systems with bodies in relative motion. Concerns have been continually raised about the accuracy of the interpolation necessary to transfer data between component grids, particularly the lack of conservation at the interfaces of the different grid blocks [4].

The approach of Cartesian grids is attractive because of its inherent simplicity and potential for automation. Many studies choose to approximate very complex geometries only by the grid lines on Cartesian co-ordinates, or the so-called saw-tooth Cartesian method in this paper. This method, even today, is widely used for large scale problems in environmental and hydraulic engineering, such as the modeling of fluid flows in the oceans and lakes [5] and heat transfer in engineering devices [6]. A structured grid and a fine grid spacing are generally utilized in this approach. Chai and Patankar [6] used this method to simulate the radiative heat transfer on a complex geometry and obtained satisfactory results. The advantage of this approach is that it is much simpler, both in the governing equations and numerical procedures, than the previous methods. One drawback of this approximation is that it forms the saw-tooth or stair-like boundary surface and the boundary will remain rough and full of angles even if the grid size is refined. This saw-tooth method is further investigated in this paper. Another classical method to treat complex geometries in Cartesian co-ordinates is the use of additional nodes from the intersection of complex geometry boundary and Cartesian co-ordinates [7]. Although this approach provides much smoother boundary approximation, it creates numerical instability in solving the system of discretized equations derived from the governing equation. This is due to the fact that some boundary nodes can become very close to the Cartesian grids. When this happens, the system of discretized equations can become very stiff and unstable and hence difficult to solve.

Recently, a multiblock unstructured Cartesian method has been used for the problems with very complex geometries [8,9]. In this approach, the grid is locally refined around the boundary through recursive subdivision with octree data structure. Aftosmis *et al.* [8] enhanced the accuracy of the boundary treatment by triangulating the portion of the surface intersected by

each Cartesian cell. This results in several triangular cells for each Cartesian boundary cell, thus greatly increasing the total number of surface triangles. While the grid generation is completely automatic once the boundary surfaces are in place, the surface triangulation is most time consuming and the operation is user-intensive, as pointed out by Aftosmis [8]. An unstructured grid is employed, therefore, this method requires more storage per grid point and prevents the exploitation of factored and directional solvers [2].

An improved method for computing flow fields involving complex geometries using a Cartesian grid was proposed by Chen *et al.* [10] and is further developed in this research. In the proposed method, complex boundaries are approximated by both Cartesian grid lines and diagonal segments in Cartesian co-ordinates. A structured Cartesian grid is employed in the approximation. The proposed method is simpler and more accurate than the traditional saw-tooth method due to the use of a structured grid and the addition of diagonal segments to approximate the boundaries. The primary goal of this method is to achieve problem-independence and automation of grid generation for problems with complex boundaries. At the same time, the emphasis is placed on improving the accuracy of geometry approximations and the corresponding fluid solutions in comparison with those of the traditional saw-tooth method. The present study is consistent with that of Thompson [2], who made a detailed review of grid generation in the 1990s, stating that the major driving factors and efforts in comprehensive grid codes must first be automation and graphical interaction.

2. DIAGONAL CARTESIAN METHOD FOR GEOMETRY APPROXIMATION

In the present study, the contour of a complex geometry is proposed to be approximated by both Cartesian grid lines and diagonal line segments as shown in Figure 1(c) and (d), respectively. The approximation that uses the proposed diagonal segments, as shown in Figure 1(d) is obviously closer to the original contour than the saw-tooth method shown in Figure 1(a) and (b).

The proposed approximation method can be used for any complex geometry. However, for complex boundaries, the approximation often cannot be made manually, especially when a large number of grids are involved. Therefore, an automatic method should be developed to approximate the given complex geometry in Cartesian co-ordinates. This is considered here. Let the original complex contour S, as shown in Figure 2, be described by a set of discretized data points. Suppose 'A' and 'B' are two neighboring contour data points given on the original contour S. Let 'a' be the Cartesian grid node approximating 'A'. Then, in order to automate the selection of the grid node 'b' on the Cartesian grid to approximate the data point 'B', the minimum distance rule is used. The distances between 'B' and the neighboring grid nodes are evaluated. The Cartesian grid node 'b' in this case has the shortest distance to 'B' and is considered as the approximated grid node of 'B'.

3. SELECTION AND PRETREATMENTS OF DISCRETIZED DATA POINTS

A complex geometry can be specified either by an analytical function or, most likely, by a set of discretized data points. For the purpose of numerical treatment, the complex boundary in this study is eventually transferred so that it is given by a set of discretized data points, even if it is initially described by an analytical function. Therefore, when a Cartesian co-ordinate is decided, one may ask if there is any rule with which a set of data may be selected from the

given discretized data points, to be the boundary grid for the computation. Also, the appropriate number of discretized data points for a given grid must be known. These two problems are investigated in the following section.

3.1. Local monotonic principle of discretized data points

Consider the solid curve 1 in Figure 3 as the original complex contour. In order to provide maximum information about the nature of the contour with least number of discretized data points, local monotonic principle is used to select the number and positions of discretized data points. The local monotonicity is defined in the following manner: for any two neighboring discretized data points, such as 'a' and 'b' on contour 1 of Figure 3, the contour segment between 'a' and 'b' should vary monotonically with respect to both x- and y-directions. This definition can also be expressed mathematically as

1. Given three points of a body contour, there is no local maximum and minimum points with respect to the x- or y-co-ordinate, or there is no point with zero first-order derivative on the segment between 'a' and 'b', except that all body data points of the segment are on either the x- or y-axis.

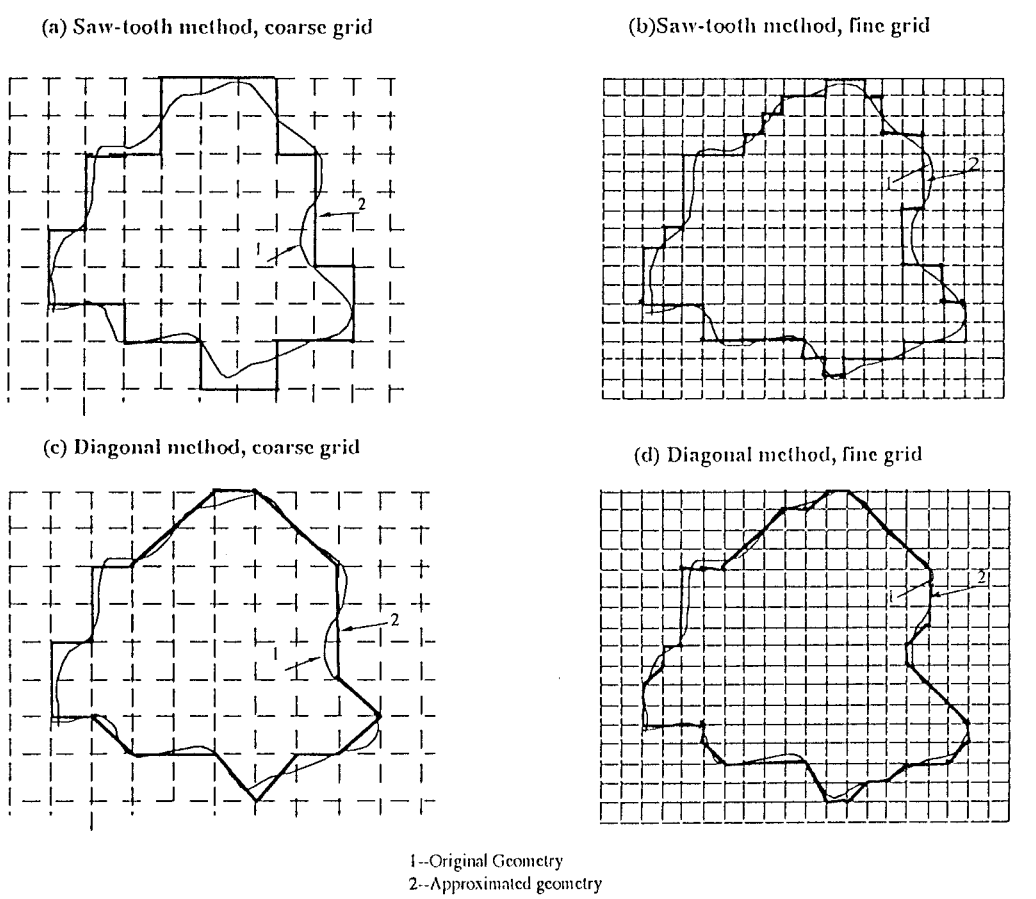

Figure 1. Approximation of complex geometries in Cartesian co-ordinates.

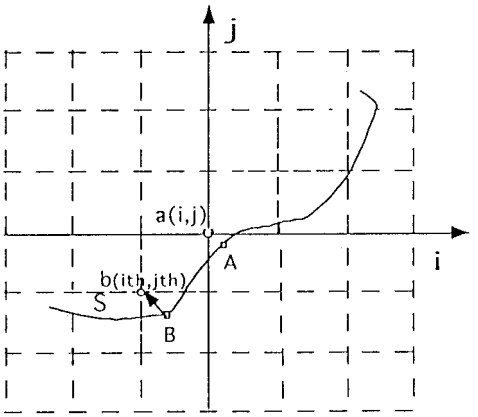

Figure 2. Approximation by shortest distance method.

2. There is no sign change of second-order derivative along the segment between 'a' and 'b' on curve 1.

Using this monotonic principle, Figure 3 shows that 20 discretized data points, such as 'a', 'b', 'c', etc. are selected as the minimum number of grid points that can adequately describe the complex contour 1. If these points are connected linearly, the dashed contour 2 is considered as an optimal approximation of the original complex contour for the number of assigned discretized data points. This is optimal because it can be found that contour 2 provides the maximum information of contour 1 with least discretized data points.

3.2. Pretreatment of discretized data points

Even if the discretized data points are properly selected by the local monotonic principle, there is still the problem of mismatch between the optimal number of discretized data points

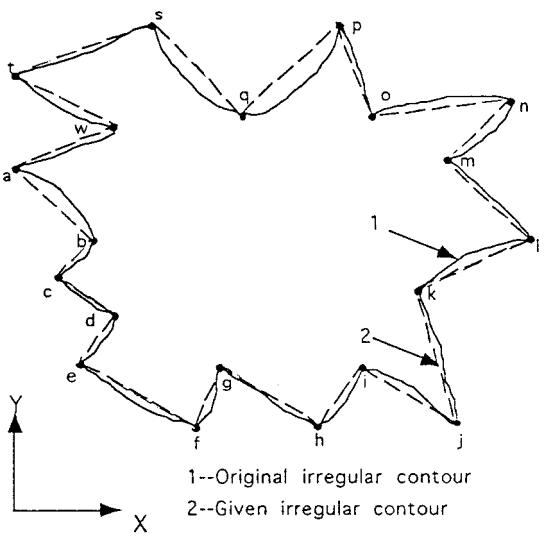

Figure 3. Principle of local monotonicity for discretized data points.

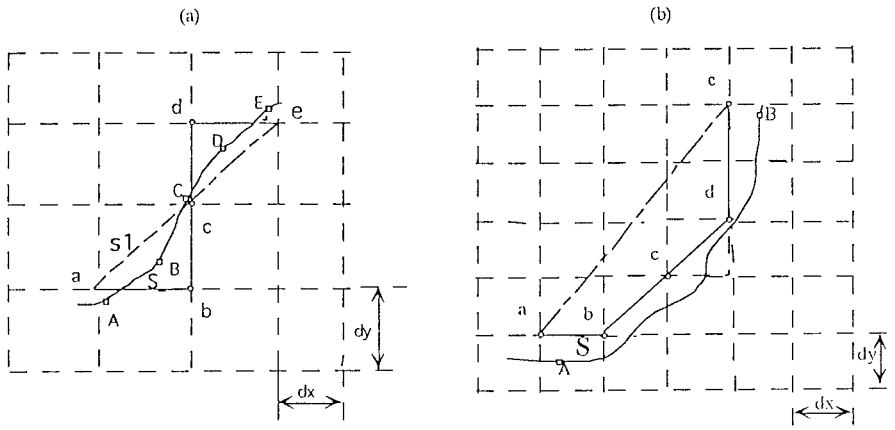

Figure 4. Pretreatment of discretized data points.

for a body contour and the number of grid points that a user has selected. This requires a pretreatment of discretized data points when a Cartesian grid size is chosen. Suppose S is one segment of the original curve contour, as shown in Figure 4(a), and the chosen grid intervals of x- and y-directions are dx and dy. As an example, five discretized data points ('A', 'B', 'C', 'D' and 'E') are specified to describe the segment S by the principle of local monotonicity. Then the corresponding approximation of S by the proposed shortest distance method is a–b–c–d–e, which turns out to be a saw-tooth-like segment. However, the ideal approximation for the given segment S would rather be S1 (a–c–e), which is closer and smoother than the approximation of a–b–c–d–e. This reveals that too many given data points in a given grid spacing may result in an undesirable approximation with many angles. In order to eliminate this mismatch phenomenon, extra data points for a body contour must be eliminated when two neighboring data points are separated by a very small distance, compared with the given grid spacing. After some numerical tests, the following criteria are adapted:

$$|x_1 - x_2| \leq 0.70\ \mathrm{d}x, \tag{1}$$

$$|y_1 - y_2| \leq 0.70\ \mathrm{d}y, \tag{2}$$

i.e. if two data points (x_1, y_1) and (x_2, y_2) meet the above two conditions, then one of these two neighboring points will be deleted.

Another problem would arise if there are not enough data points in the description of the original complex contour for a given grid spacing. Figure 4(b) shows that for the given segment S with only two given data points A and B, a straight line a–e would be the approximation of the segment S on the corresponding grid. If there are enough data points available for the body contour, the approximation with a–b–c–d–e would be obtained. Apparently, the latter one with a–b–c–d–e looks better than the straight line a–e. In this case, a linear or quadratic interpolation is used to obtain one or several extra points once two neighboring data points are found to be too far away. After some numerical tests two conditions are adapted:

$$|x_1 - x_2| \geq 1.40\ \mathrm{d}x, \tag{3}$$

$$|y_1 - y_2| \leq 1.40\ \mathrm{d}y, \tag{4}$$

i.e. if two data points (x_1, y_1) and (x_2, y_2) meet the above two conditions, at least one additional body data will be specified.

4. ACCURACY OF GEOMETRY APPROXIMATION

From the above description, the complex contour can now be approximated by both diagonal segments and grid lines. It is evident that the approximation by the saw-tooth method is still full of right angles and looks rough even if the grid is refined, while the proposed method utilizing diagonal segments may eliminate many of the right angles. Therefore, the proposed diagonal Cartesian method will give a more close approximation than the saw-tooth method. In the following, the accuracy of both the proposed diagonal and the saw-tooth approximations are considered.

It is obvious that in a good approximation of a complex geometry the contour should be as close as possible to the original one. It appears to be possible to use the least square method for the accuracy estimation of the geometry approximations. However, both the original contour and the approximated one are generally so complex that they cannot be described by the analytic functions. Instead, they are described by two sets of discretized data points at different locations. Therefore, the technique of the least square method using the distances separating the original and approximated contours cannot be easily implemented in the present accuracy estimation of the geometry approximation.

In the following sections, the accuracy of the approximation is estimated quantitatively by the following two criteria, based on the concept of the least square method.

4.1. Relative length errors E1

Since both the original and the approximated contour are described by two sets of discretized data points, the concept of relative error of total lengths $E1$ between the two contours can be calculated as follows.

Consider solid curve 1 and dashed curve 2 in Figure 5, which are the original and the approximated contours, respectively. They are described by two sets of discretized data points, such as 'A', 'B' and 'a', 'b' in Figure 5. Let $L\mathrm{O}$ and $L\mathrm{A}$ be the total length of the original and approximated contour, respectively. They can be calculated in the following ways:

$$L\mathrm{O} = \sum_{i=1}^{n\mathrm{o}} (\Delta l_{\mathrm{o}})_i, \tag{5}$$

$$L\mathrm{A} = \sum_{i=1}^{n\mathrm{a}} (\Delta l_{\mathrm{a}})_i, \tag{6}$$

where

$$(\Delta l_{\mathrm{o}})_i = \sqrt{(\Delta x_{\mathrm{o}})_i^2 + (\Delta y_{\mathrm{o}})_i^2}, \tag{7}$$

$$(\Delta l_{\mathrm{a}})_i = \sqrt{(\Delta x_{\mathrm{a}})_i^2 + (\Delta y_{\mathrm{a}})_i^2}. \tag{8}$$

In the above equations, $n\mathrm{o}$ and $n\mathrm{a}$ are the numbers of discretized data points on the original and approximated contours, respectively. Δx and Δy are the differences of x- and y-co-ordinates for two neighboring nodes, such as 'A' and 'B' on the original contour and 'a' and 'b' on the approximated contour in Figure 5.

After LO and LA are evaluated, the relative error of total length $E1$ is defined as

$$E1 = \frac{|LO - LA|}{LO} \times 100\%. \tag{9}$$

A good approximation of the original complex contour is expected to have a small value of relative length error $E1$. Therefore, the proposed diagonal approximation should have a smaller value of $E1$ than that of the saw-tooth approximation. This prediction is verified in later sections.

4.2. Average normal distance E2

The sharp edges on a boundary will lead to flow separations and vortical development in the nearby regions. Therefore, large normal distances between the original and approximated boundaries mean that large errors will be brought in the numerical solutions of fluid flows around the approximated boundaries. In order to ensure that an approximate contour is appropriate, a method to verify the separation of the original and approximated contours must be found.

Consider Figure 5(a), where the approximated contour is described by a set of discretized grid nodes, such as 'a' and 'b'. The normal distances from approximated grid nodes to the original contour 1, denoted as 'am' in Figure 5(a,b), should be small for a good approximation. It should be pointed out that since the original contour 1 is described by a set of discretized data points, 'an' rather than 'am' will be used numerically to represent the normal distance from 'a' to the original contour 1, where 'an' is normal to AB. Using the characteristic length of the computational domain LD as a reference length, a dimensionless average normal distance $E2$ can be defined by

$$E2 = \frac{AND}{LD}. \tag{10}$$

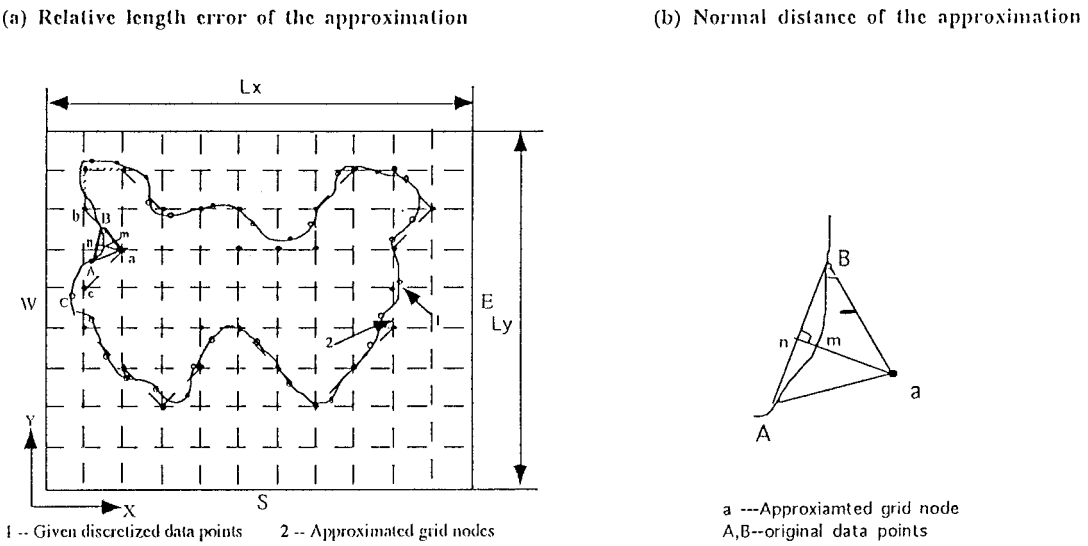

Figure 5. Evaluation of approximation accuracy for complex geometries.

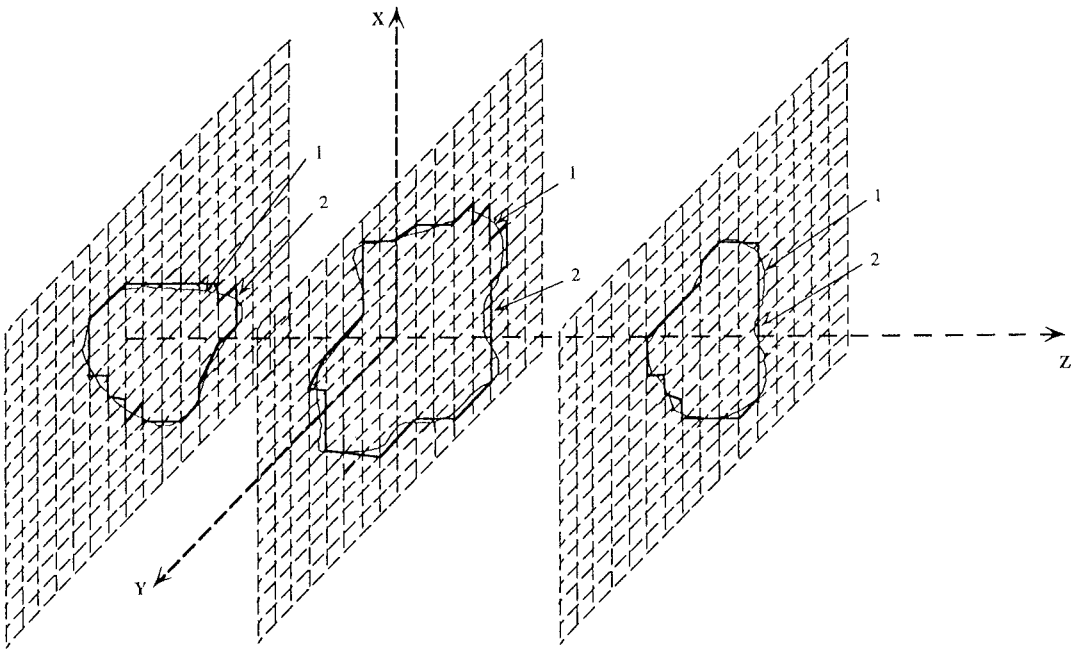

Figure 6. Approximation of three-dimensional complex boundaries.

In the above equation, AND is the average normal distance and can be evaluated from

$$AND = \frac{\sum_{i=1}^{n\mathrm{a}} (\mathrm{a}n)_i}{n\mathrm{a}}, \tag{11}$$

where na is the number of grid nodes on the approximated contour and an is the absolute normal distance from 'a' to the original contour 1. In this paper, the characteristic length is given by

$$L\mathrm{D} = \frac{(Lx + Ly)}{2}, \tag{12}$$

where Lx and Ly are the characteristic lengths of the body domain shown in Figure 5(a). $E2$ is another criterion to test the suitability of the approximation.

5. APPROXIMATIONS OF THREE-DIMENSIONAL COMPLEX GEOMETRIES IN CARTESIAN CO-ORDINATES

One of the challenging problems in simulating the fluid flows around three-dimensional complex geometries is the automatic grid generation for the complex boundaries. In this research, the diagonal Cartesian method described for the approximation of two-dimensional complex contours in the above sections can be extended to treat the three-dimensional complex geometries in Cartesian co-ordinates. Following are the general procedures:

1. On the same Cartesian co-ordinate, the three-dimensional complex geometries are sliced along one co-ordinate axis (such as the Z-axis in Figure 6) and expressed by a series of two-dimensional contours which are parallel to each other and perpendicular to the Z-axis. A finer grid along the Z-direction means that more slices are used to describe the original three-dimensional complex boundary.
2. On each slice, the techniques discussed in the above sections are employed to approximate the two-dimensional complex contour.
3. After finishing the approximation of two-dimensional complex contours on all slices the three-dimensional complex boundary is then successfully approximated by a three-dimensional surface which is made up of a series of Cartesian grid nodes in the same Cartesian co-ordinate.

6. APPROXIMATIONS OF TWO-DIMENSIONAL COMPLEX GEOMETRIES

In order to illustrate the proposed approximation method, a number of two-dimensional complex geometries are approximated by the proposed method and compared with that approximated by the conventional saw-tooth method. Different grid sizes are used to determine the relative error of $E1$ and average normal distance $E2$ for some approximations. All approximations are automatically generated once the contour data points and the grid size are given and specified. Error estimations are also automatically calculated.

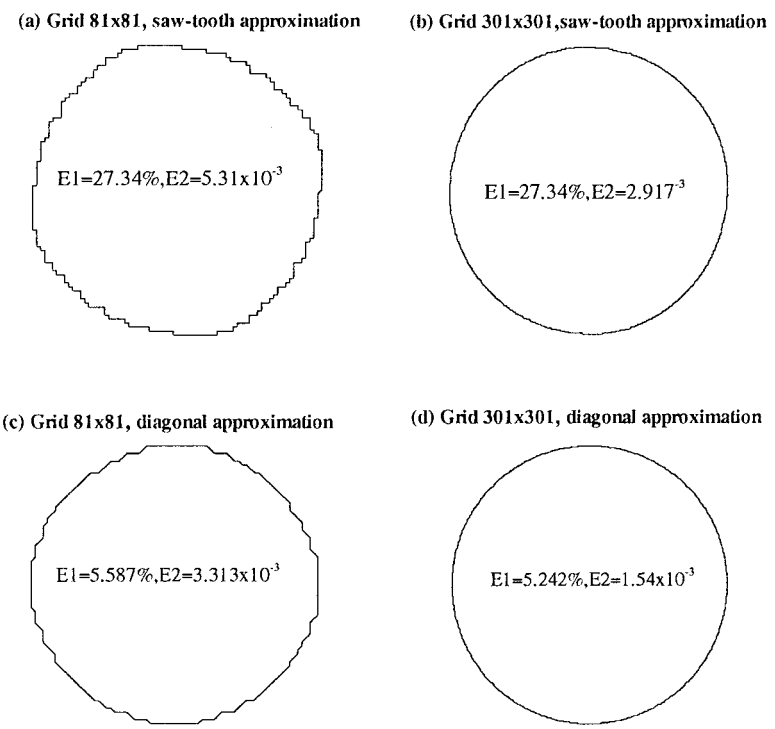

Figure 7. Approximation of circles.

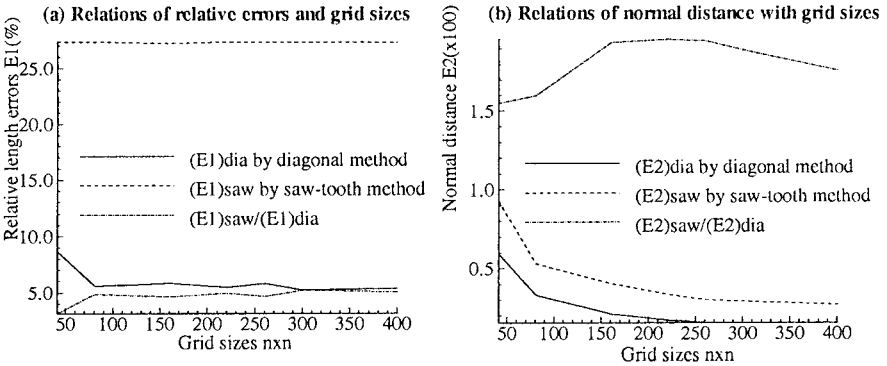

Figure 8. Accuracy of circle approximation.

6.1. *Approximation of single complex geometries*

Figures 7–12 give the approximations of complex geometries in Cartesian co-ordinates and the accuracy estimations of $E1$ and $E2$.

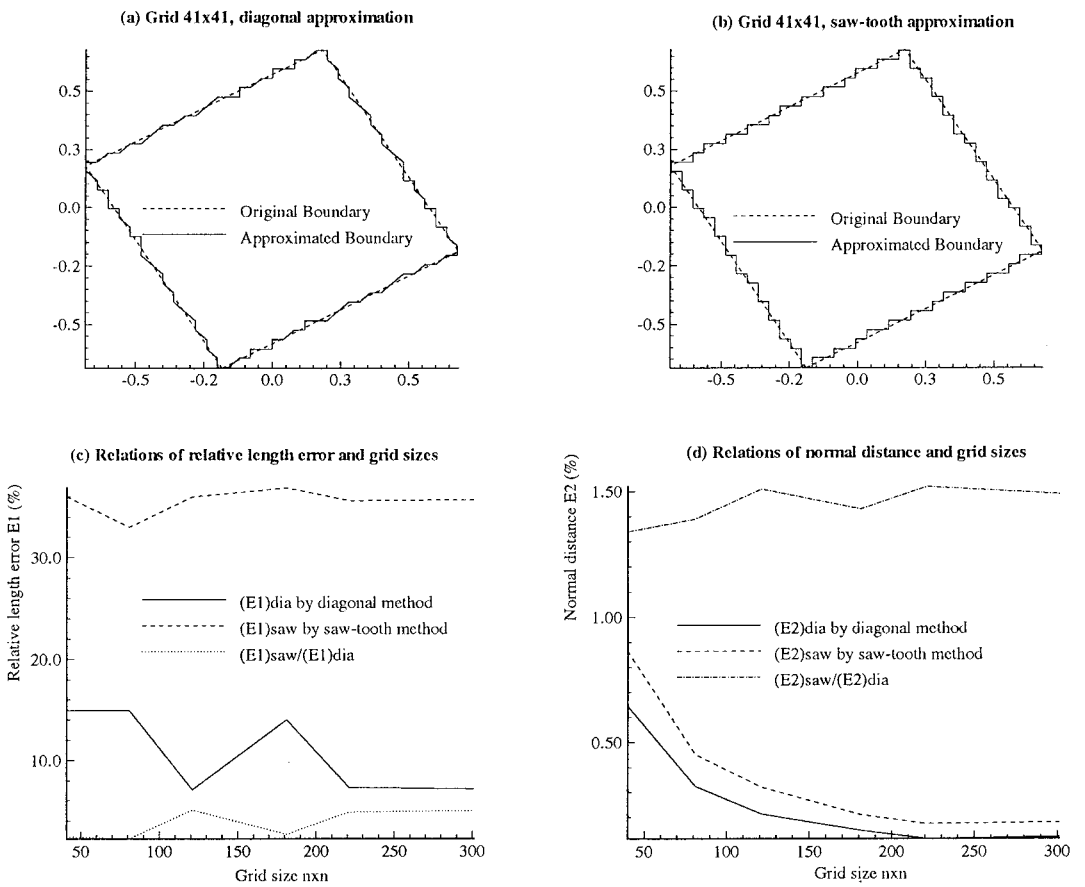

Figure 9. Approximation of a rotated cavity.

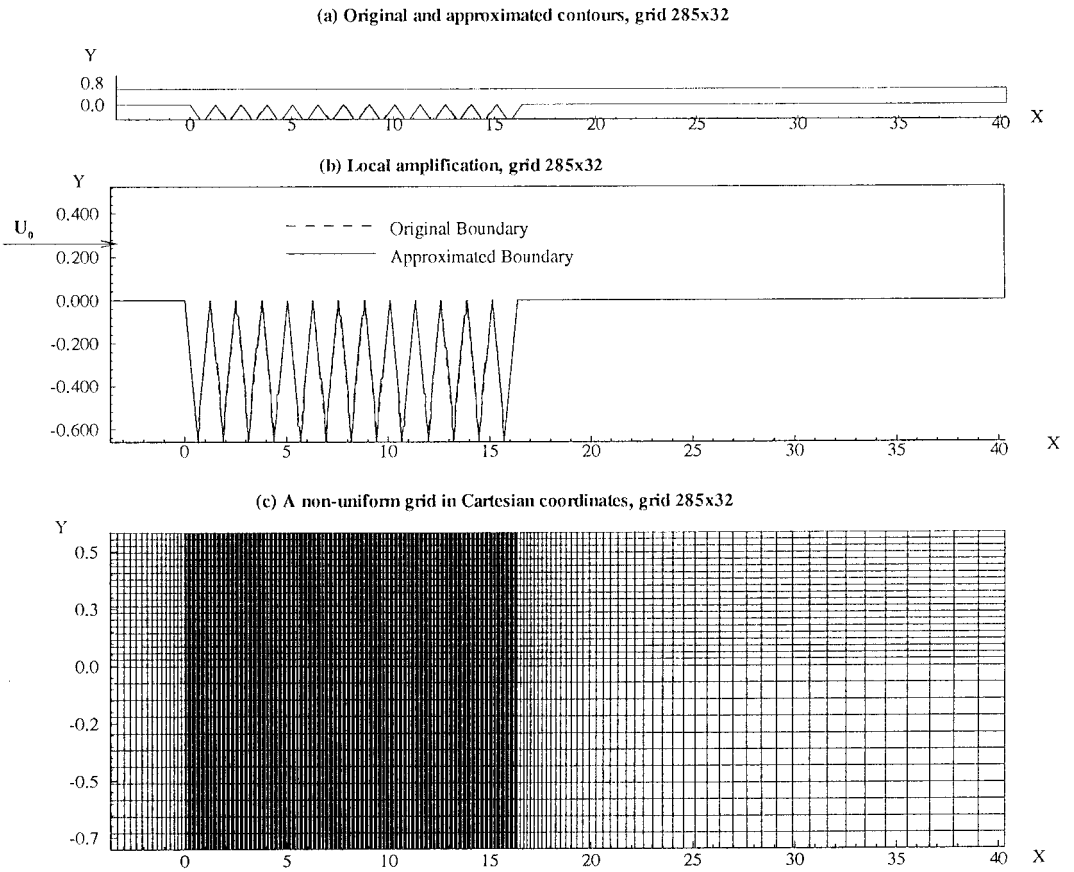

Figure 10. Approximation of a grooved channel.

The fluid flow around a cylinder is a classical topic in computational fluid dynamics (CFD). In a Cartesian grid, a circle becomes a complex geometry, and is considered in this research to test the validity and robustness of the proposed diagonal method. Figure 7(a) and (c) respectively, show the approximations of circle obtained by the saw-tooth approximation and the proposed diagonal method at the same grid. The approximation made by the saw-tooth

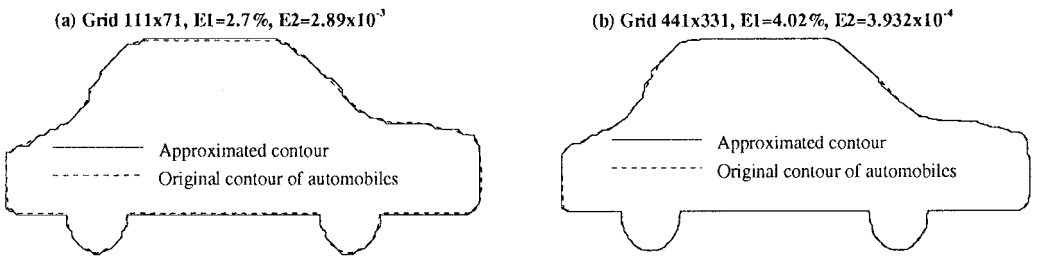

Figure 11. Approximation of automobiles.

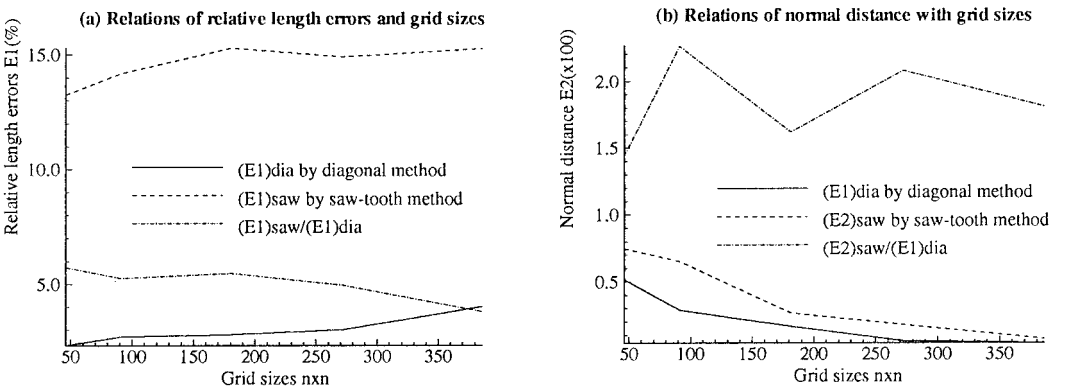

Figure 12. Accuracy of approximation for automobiles.

method has the relative length error $E1$ of 27.34% and the average normal distance $E2$ of 5.31×10^{-3}, while the proposed diagonal approximation has only the relative length error $E1$ of 5.587% and the average normal distance $E2$ of 3.313×10^{-3}. Figure 7(b,d) gives the approximations made by a finer grid (301×301).

Again, it shows that saw-tooth approximation has higher relative length error and average normal distance ($E1 = 27.34\%$, $E2 = 2.917 \times 10^{-3}$) than the diagonal approximation method ($E1 = 5.24\%$, $E2 = 1.54 \times 10^{-3}$). In Figure 8, the relations of relative length errors $E1$ and average normal distance $E2$ with grid sizes are shown. As expected, the relative length errors shown in Figure 8(a) for the saw-tooth approximation are about four to five times larger than that by the proposed diagonal approximation. Figure 8(b) shows that both ($E2$)saw and ($E2$)dia decrease with the grid size. As expected, ($E2$)saw is about twice as large as ($E2$)dia.

The fluid flow in a lid-driven cavity is used as a benchmark problem for the verification of the diagonal method in this research. If a cavity is rotated with respect to the Cartesian co-ordinates, as shown in Figure 9, the rotated cavity presents a complex contour in Cartesian grids. In Figure 9(a,b) the cavity is rotated by 30° with respect to the original x-axis. A grid size of 41×41 is used for the approximations by both the diagonal and saw-tooth methods. Figure 9(c,d) shows that the diagonal method gives smaller values of $E1$ and $E2$.

In order to enhance the heat transfer in a channel flows, a channel has been grooved [11], as shown in Figure 10(a). The boundary of the grooved channel is very complex, even for the boundary-fitted co-ordinates, due to the sharp edges in the channel. Figure 9(a,b) gives the approximation of the grooved channel in Cartesian co-ordinates. A non-uniform grid of 285×32 is utilized in the approximation. It is found that an excellent geometry approximation has been obtained by the proposed diagonal Cartesian method.

The approximation of automobile surface and the lake bank in the Cartesian co-ordinate are also studied here because the simulation of fluid flows and heat transfer around automobiles and in lakes are of interest in the automobile industry and hydraulic and environmental engineering. Figure 11 shows the approximation of an automobile by the proposed method. The original automobile contour is given by the dashed line. Although there is a difference between the original geometry and the approximated geometry with a grid size of 111×71 (Figure 11(a)), the relative length error $E1$ and average normal distance $E2$ are relatively small ($E1 = 2.7\%$ and $E2 = 2.89 \times 10^{-3}$). When the grid size is increased from 111×71 to 441×331, a more satisfactory approximation is obtained, as shown in Figure 11(b). The accuracy analysis is given in Figure 12. Again, the relative length errors $E1$ and average normal distance

$E2$ for the saw-tooth approximation method are found to be larger than those of the diagonal approximation. Also, average normal distance $E2$ becomes smaller with a finer grid.

In Figure 13, the given lake bank is very complicated and is described by 101 discretized data points. The dashed line represents the original complex lake bank. Two different grid sizes of 81×81 and 301×301 are used here. Examining the figure, it is seen that for the lake bank with slopes around 45°, or the so-called diagonal boundaries, the diagonal approximation is obviously much closer to the original contour than the saw-tooth approximation. This shows the advantage of diagonal approximation. For the saw-tooth approximation, the approximated lake bank is full of angles and rough corners, even when the grid size is increased from 81×81 to 301×301, while the approximation by the proposed diagonal method rapidly approaches the original complex lake banks when the grid is refined. This means the saw-tooth method is not convergent in the geometry approximation. This phenomenon can be further verified by the relative length errors $E1$ and average normal distance $E2$ shown in Figure 14. It is also found that both $(E1)$saw and $(E2)$saw are larger than $(E1)$dia and $(E2)$dia.

6.2. *Approximation of multicylinder*

Figure 15 shows the automated approximation of multicylinders by the proposed method in Cartesian grids. It should be noted that the generation of boundary-fitted co-ordinates for the multibody contours is generally very difficult with currently available techniques [12]. How-

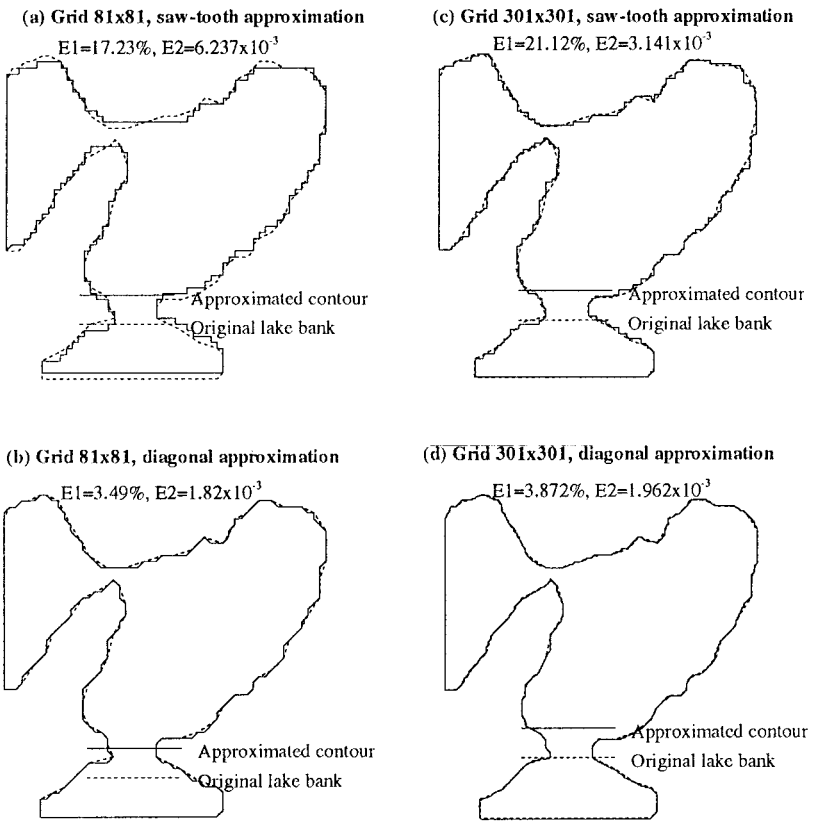

Figure 13. Approximation of lake banks.

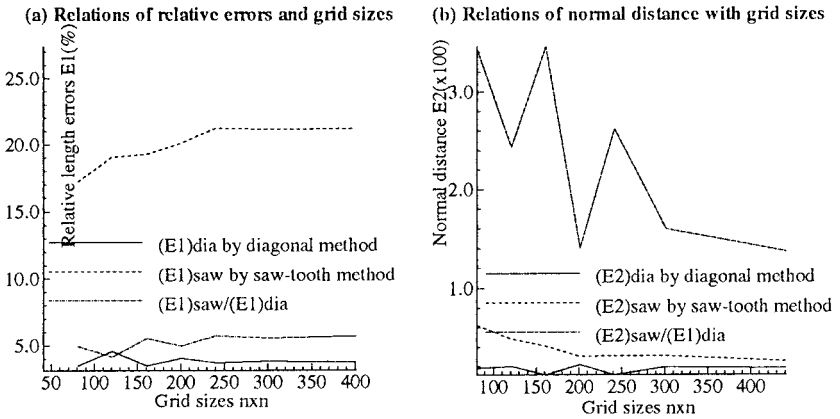

Figure 14. Accuracy of lake banks.

ever, it is easy with the proposed diagonal approximation method, due to the employment of an automated structured Cartesian co-ordinate. In order to examine an accurate approximation of a multibody system, a coarse grid (141×141) and a fine grid (501×501) are employed here. Excellent approximation is achieved with the fine grid.

6.3. Complex geometries in porous media

The numerical simulation of the fluid flows and the conjugate heat transfer around complex geometries, such as those in the porous media (Figure 16(b)), remains a very challenging problem in CFD. The key point for this problem is how to treat such complicated and multibody geometries. Figure 16(a,c) shows the approximations of the porous media geometries in Cartesian co-ordinates by both diagonal and saw-tooth methods. It shows that

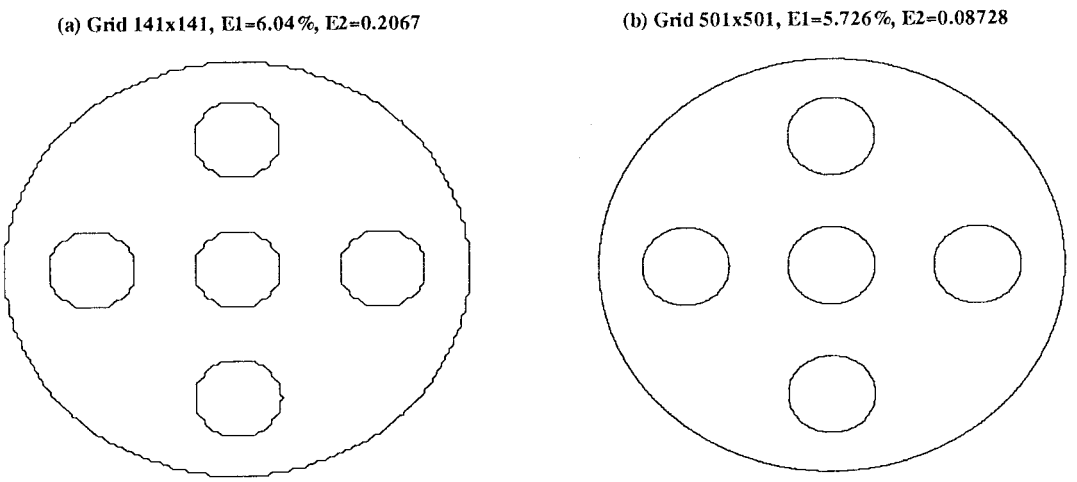

Figure 15. Diagonal approximation of multicylinder.

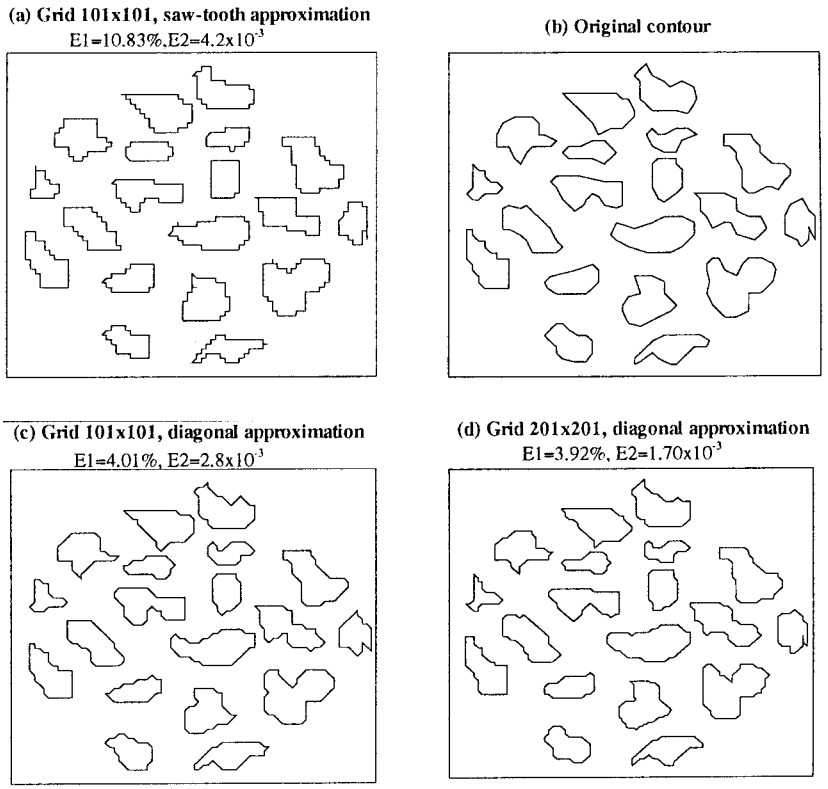

Figure 16. Diagonal approximation of complex contours in porous media.

although the same grid size (101×101) is utilized, the diagonal approximation gives a much close approximation than that by the saw-tooth method, which can also be verified by the values of relative length error $E1$ and average normal distance $E2$. When the grid is refined to 201×201, a quite reasonable approximation is obtained by the proposed diagonal method and the average normal distance is reduced to a value of 1.7×10^{-3}.

7. APPROXIMATIONS OF THREE-DIMENSIONAL COMPLEX GEOMETRIES

The grid generation for complex three-dimensional boundaries are very difficult with current available methods, especially for the automation of grid generation. Based on the two-dimensional approximations in Figures 10 and 13, the approximations of a three-dimensional grooved channel and a lake bank in Cartesian co-ordinates are given in Figures 17 and 18, respectively. It is obvious that the diagonal treatment gives the diagonal walls in these approximations, which is impossible with the saw-tooth method.

Figure 19 shows the approximations of a sphere in a structured Cartesian grid by both diagonal and saw-tooth methods. A grid of $121 \times 121 \times 31$ is employed. Obviously the diagonal approximation is much more smooth than the saw-tooth approximation, which can be further explained by the accuracy estimations in Figure 8.

8. VERIFICATION OF THE DIAGONAL METHOD AND ITS APPLICATION

This section first describes the verifications of the proposed diagonal method and its improvement in fluid solutions compared with the saw-tooth method. The problem of a lid-driven cavity is chosen, as it has been widely used as a benchmark problem in CFD since Ghia *et al.* [13] published the numerical solution by the multigrid method in 1982. Then the application of the proposed diagonal method in the prediction of a grooved channel is given.

8.1. Solutions of a rotated lid-driven cavity flow

A rotated cavity presents a complex contour in Cartesian grid, as shown in Figures 9 and 20(a). The fluid flow inside this rotated lid-driven cavity at Reynolds number of 1000 is used for the verification of the proposed diagonal method in Figure 20. The detailed numerical approaches are not given here since this paper is about the grid generation of complex geometries. The effective grid size stated in Figure 20(a) means the actual grid number inside the cavity, since there is a solid domain outside the cavity. The grid sizes in Figures 20 and 21 are all effective grid numbers. Nine-point and five-point finite analytic schemes are utilized to discretize the Navier–Stokes equations on regular and irregular elements, respectively [10,14]. Figure 20 gives the central velocity distributions and the convergent history. It is shown that the solution of this lid-driven cavity flow is in excellent agreement with that obtained by Ghia *et al.* [13].

It should be pointed out that the co-ordinates in Figure 20(c,d) 21 are different from that in Figure 20(a), since the relative distances from the walls are used in the measurement of x- and y-co-ordinates in those figures, i.e. the central velocity along the central lines of y_0y_1 and x_0x_1 in Figure 20(a) are presented. Also, U and V in Figures 20 and 21 are the central velocities along the directions of X and Y, as shown in Figure 20(a). By the diagonal method, the central

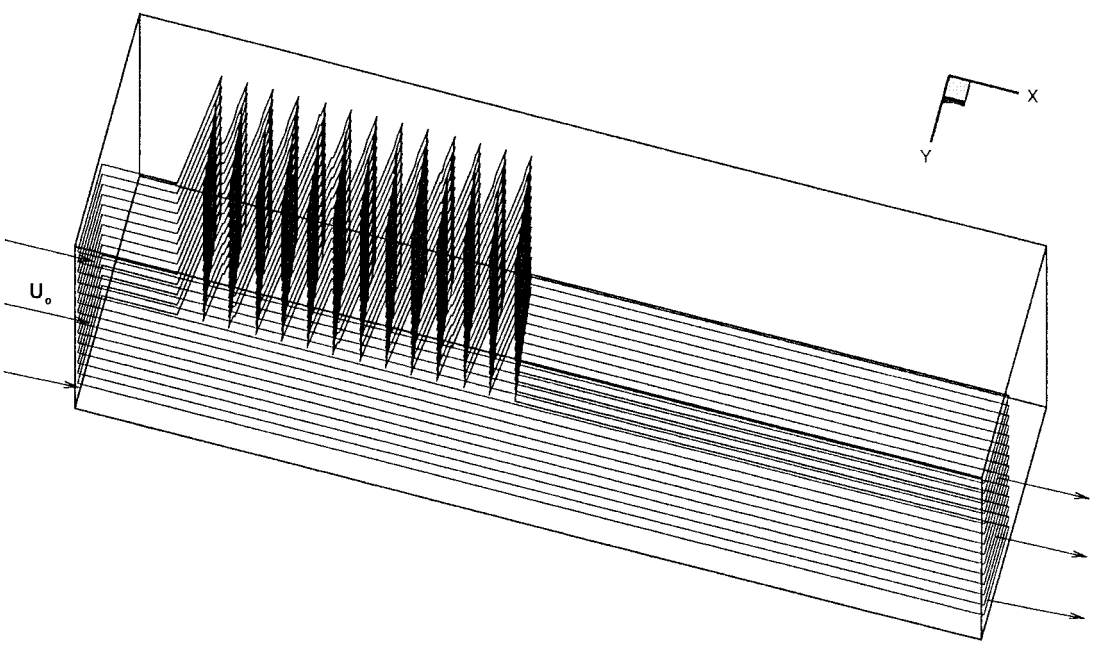

Figure 17. Approximation of a grooved channel in Cartesian co-ordinates (grid $285 \times 32 \times 14$).

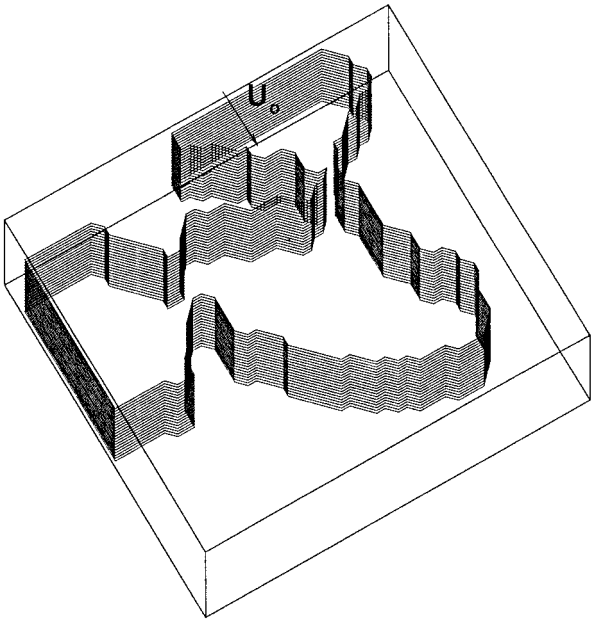

Figure 18. Approximation of a lake bank in Cartesian co-ordinates (grid $41 \times 61 \times 25$).

velocities of U and V using a single uniform grid with a grid size of 144×144 are in good agreement with the results of Ghia *et al.*, who used a multigrid with a grid size of 129×129. Different grid sizes are tested for the grid independence of the solutions in Figure 20(c,d). Figure 20(b) gives the residual history of pressure and velocities at the last time step and it

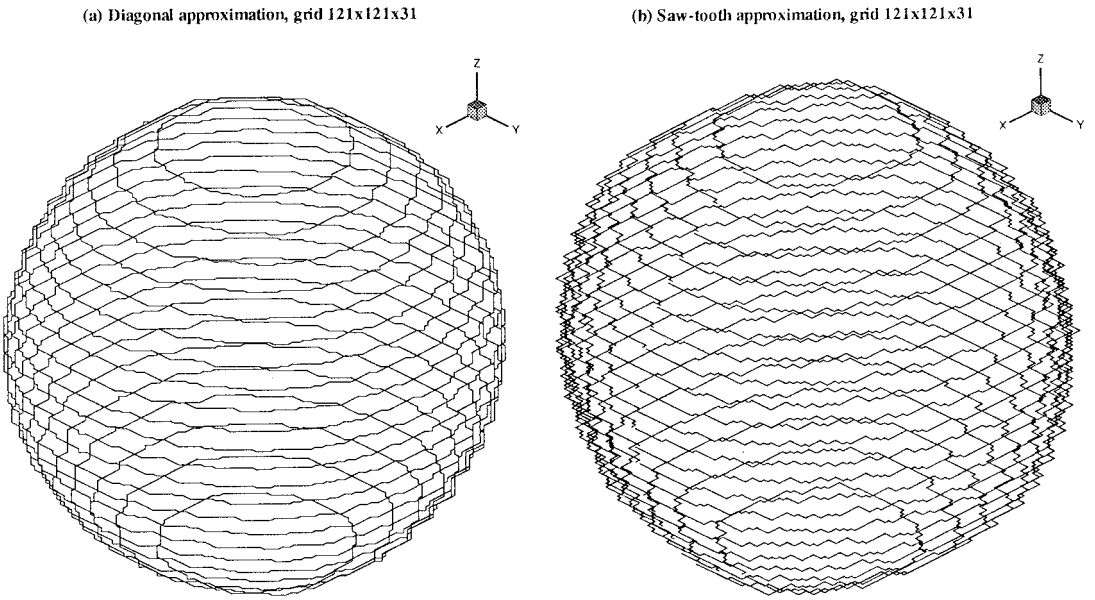

Figure 19. Approximation of sphere in Cartesian co-ordinates.

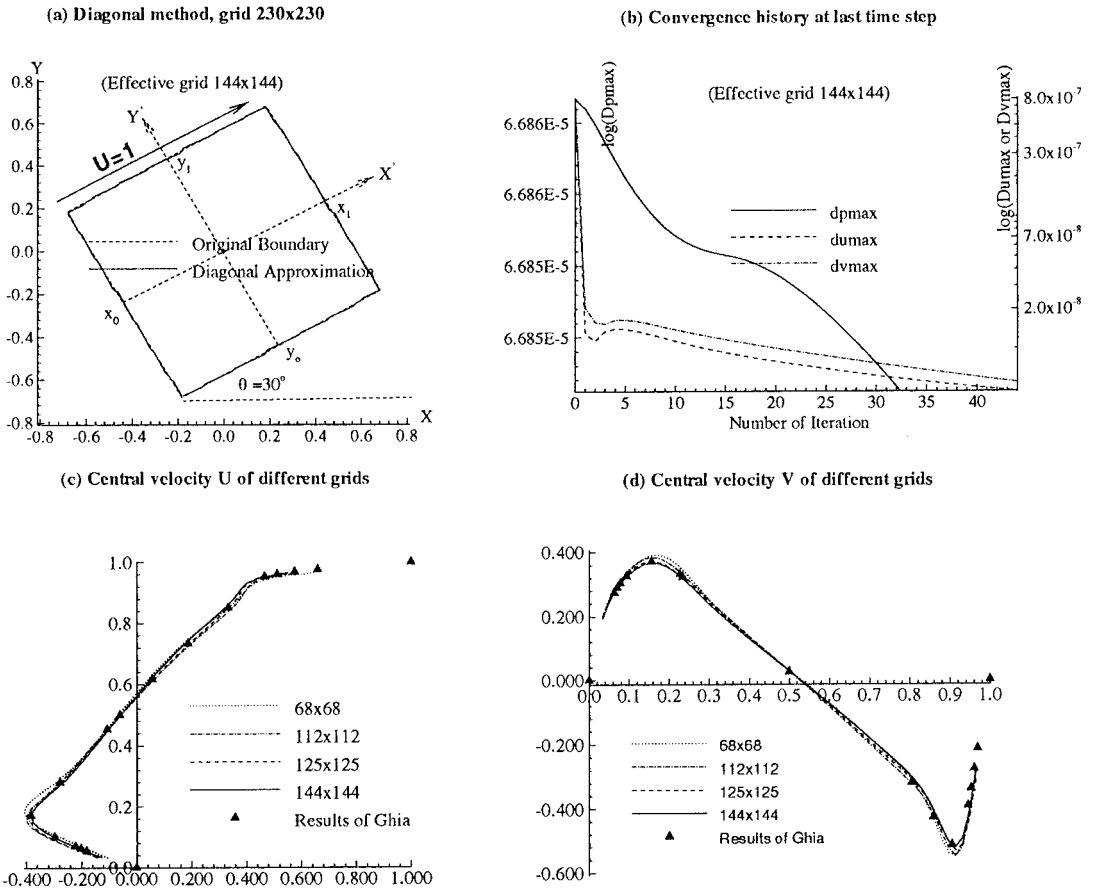

Figure 20. Solutions of a rotated cavity flow by diagonal method ($Re = 1000$).

shows good convergence. The variables of $\mathrm{d}p_{\max}$, $\mathrm{d}u_{\max}$ and $\mathrm{d}v_{\max}$ are the residuals of pressure and velocity fields during the iteration and are given by

$$\mathrm{d}p_{\max} = \max(P_{i,j}^{n} - P_{i,j}^{n-1}), \tag{13}$$

$$\mathrm{d}u_{\max} = \max(U_{i,j}^{n} - U_{i,j}^{n-1}), \tag{14}$$

$$\mathrm{d}v_{\max} = \max(V_{i,j}^{n} - V_{i,j}^{n-1}), \tag{15}$$

where i and j are grid point indices which range from 1 to $i_{\max}$ and $j_{\max}$, respectively. n and $n-1$ are the present and previous time steps. Thus, the residual for each variable is simply the maximum difference, over the entire computational domain, between the values of that variable at the present and previous time steps. Therefore, it is demonstrated that the diagonal method gives convergent, grid-independent and stable solution for the rotated lid-driven cavity flow.

Figure 21(c,d) shows the solution of a rotated lid-driven cavity flow by the saw-tooth method. It is interesting that the saw-tooth method underpredicts the central velocities at fine grids and overpredicts the central velocities at coarse grids. Although velocity fields converge, the pressure field diverges by the saw-tooth method, except for the solution at the grid size of

112×112, probably due to the failure of mass conservation close to the lid-driven boundaries. This is consistent with the situation where the geometry approximation of lake bank by the saw-tooth method is not convergent, i.e. the boundary of the lake bank still remains rough and full of angles even when the grid is refined, as shown in Figure 13. Figure 21(a,b) shows the differences of solutions by both diagonal and saw-tooth methods at the same grid size of 144×144. It is obvious that the prediction of this rotated cavity flow is greatly improved by the diagonal method, compared with the results obtained with the saw-tooth method.

8.2. Solutions of the flow in a grooved channel

It has been found experimentally that the heat transfer can be improved in a grooved channel in comparison with a smooth channel [11]. This grooved channel presents a very complex geometry for numerical analysis due to its sharp edges. Figure 10 gives the diagonal approximation of a grooved channel in a non-uniform grid. The corresponding numerical solution at Reynolds number of 100 is shown in Figure 22. The Reynolds number is based on the entrance height and the average velocity at the entrance section. The streamfunction in Figure 22(b) indicates that there are small vortices inside the grooved area. It is due to these vortical movements that the heat transfer between the fluid inside the channel and the solid at

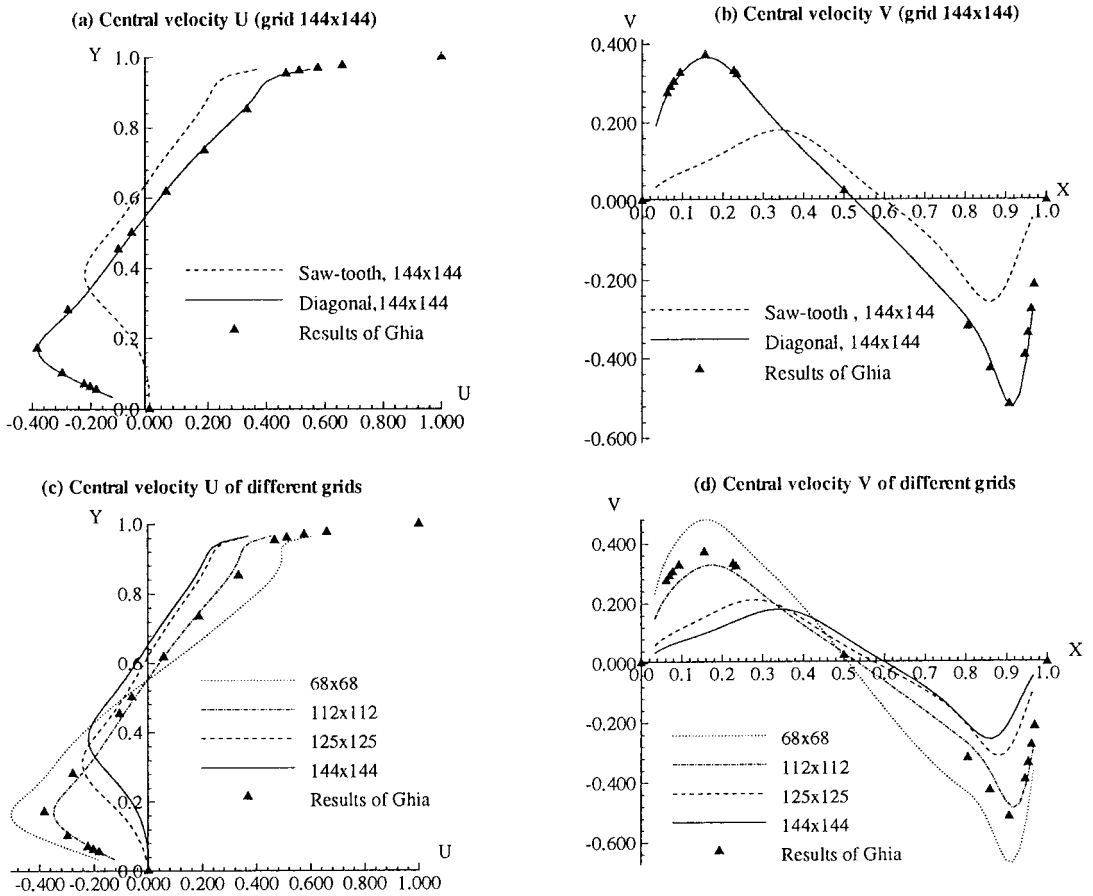

Figure 21. Solutions of a rotated cavity flow by saw-tooth method ($Re = 1000$).

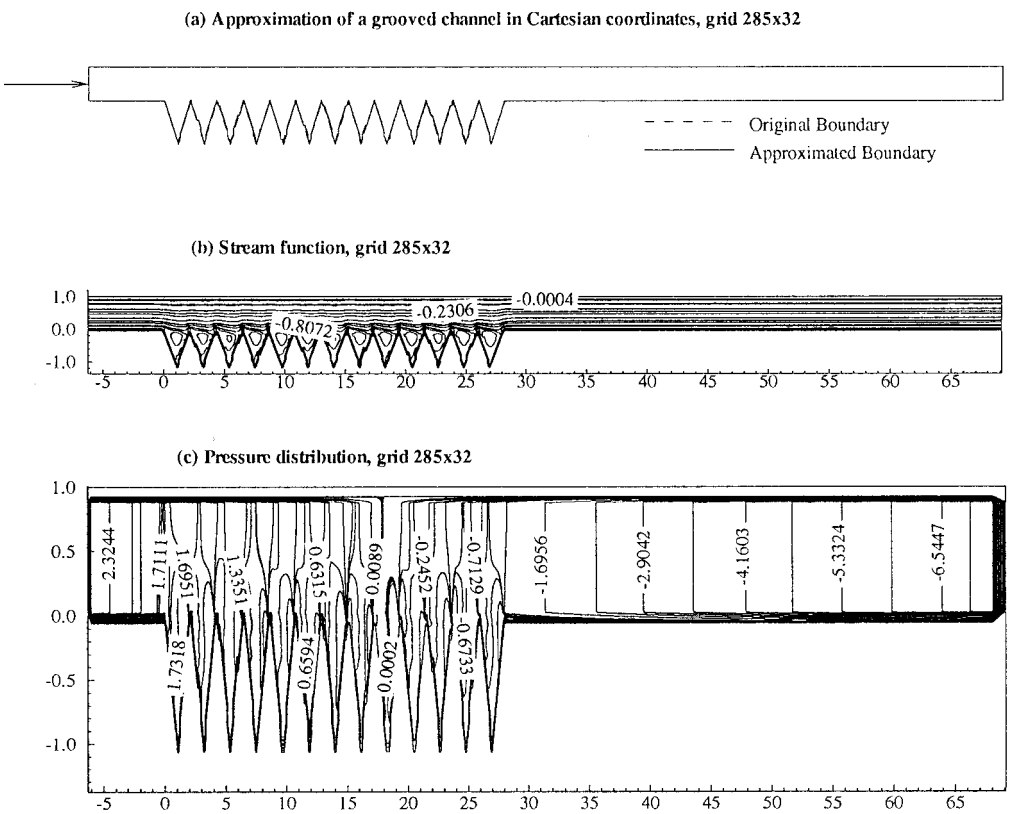

Figure 22. Solutions of a grooved channel flow ($Re = 100$).

the channel walls is enhanced. From the streamlines, it is found that only the flows close to the grooved area are disturbed because of the low Reynolds number. The streamlines at the top of channel remain almost straight. This implies that the flow in these areas is not disturbed by the presence of the groove. It is expected that the disturbed areas will be expanded further into the channel at a higher Reynolds number. The pressure distributions are also shown in Figure 22(c). Again, the pressure near the top wall of the channel is almost unaffected. Similar to a smooth channel flow, the pressure drops toward the downstream direction.

9. CONCLUSIONS

This paper proposes a method for the approximation of complex geometries with both grid lines and diagonal segments in Cartesian co-ordinates. The proposed method allows automatic grid generation. The accuracy of the geometry approximation is examined. It shows that the diagonal method gives less error in comparison with the error obtained by the traditional saw-tooth method. The diagonal method is easy to implement numerically because a structured grid is utilized. The analysis of relative length errors and average normal distance for the geometry approximation shows the validity of the diagonal approximation. The numerical solution of a rotated cavity flow proves that the diagonal Cartesian method gives a stable, convergent and grid-independent solution, while the traditional saw-tooth method gives either

the divergent solution or the result with a large error. The numerical result of a grooved channel shows that this diagonal method is capable of handling real engineering problems with very complex geometries.

ACKNOWLEDGMENTS

The authors would like to thank SCRI (Supercomputer Computations Research Institute) at Florida State University for the use of their computer facilities in this research.

REFERENCES

1. J.F. Thompson, F.C. Thames and C.W. Mastin, 'Automatic numerical generation of body-fitted curvilinear coordinate system for field containing any number of arbitrary two-dimensional bodies', *J. Comput. Phys.*, **15**, 299–319 (1974).
2. J.F. Thompson, 'A reflection of grid generation in the 90s: trends, needs, and influences', in B.K. Soni, J.F. Thompson, J. Hauser and P. Eiseman, (eds.), *5th Int. Conf. Numerical Grid Generation in Computational Field Simulations*, Mississippi, USA, pp. 1029–1110, April 1–5, 1996.
3. J.F. Baker, *Finite Element Computational Fluid Mechanics*. McGraw-Hill, New York, 1983.
4. D.M. Belk, 'The role of overset grids in the development of the general purpose CFD code', in *Proc. Surface Modeling, Grid Generation and Related Issues in Computational Fluid Dynamics Workshop*, NASA Lewis Research Center, Cleveland, OH, NASA Conference Publication 3291, p. 193, May 1995.
5. K. Nakatsuji, T. Sueyoshi, and K. Muraoka, 'Numerical experiments of residual circulation and its formulation mechanism in tidal estuary', in *Proc. 5th Int. Symp. Refined Flow Modelling and Turbulence Measurements*, Paris, France, pp. 695–702, September 7–10, 1993.
6. J.C. Chai, H.S. Lee, and S.V. Patakar, 'Treatment of irregular geometries using a Cartesian coordinates finite-volume radiation heat transfer procedure', *Numer. Heat Transf., Part* B, **26**, 179–197 (1994).
7. L. Lapidus and G.F. Pinder, *Numerical Solution of Partial Differential Equations in Science and Engineering*, Springer, New York, 1982.
8. M.J. Aftosmis, J.E. Melton and M.J. Bergerm, 'Adaption and surface modeling for Cartesian mesh methods', in *AIAA-95-1725-CP, 12th AIAA Computational Fluid Dynamics Conference*, San Diego, CA, June 1995.
9. M.J. Aftosmis, 'Emerging CFD technologies and aerospace vehicle design', in *Proc. Surface Modeling, Grid Generation and Related Issues in Computational Fluid Dynamics Workshop*, NASA Lewis Research Center, Cleveland, OH, NASA Conference Publication 3291, p. 359, May 1995.
10. W.F. Tsai, C.J. Chen and H.C. Tien, 'Finite analytic numerical solutions for unsteady flow with irregular boundaries', *J. Hydraul. Eng.*, **119**, 1274–1298 (1993).
11. M. Greiner, R.F. Chen and R.A. Wirtz, 'Enhanced heat transfer/pressure drop measured from a flat surface in a grooved channel', *J. Heat Transf.*, **113**, 498–501 (1991).
12. N.A. Patankar and H.H. Hu, 'Two-dimensional periodic mesh generation', in B.K. Soni, J.F. Thompson, J. Hauser and P. Eiseman (eds.), *5th Int. Conf. Numerical Grid Generation in Computational Field Simulations*, Mississippi, USA, pp. 1175–1184, April 1–5 1996.
13. U. Ghia, K.N. Ghia and C.T. Shin, 'High-*Re* solutions for incompressible flow using the Navier–Stokes equations and a multigrid method', *J. Comput. Phys.*, **48**, 387–411 (1982).
14. C.J. Chen, H. Naseri-Neshat and K.S. Ho, 'Finite analytic numerical solution of heat transfer in two-dimensional cavity flow', *Numer. Heat Transf.*, **4**, 179–197 (1981).

